Relaxation fluctuations about an equilibrium in quantum chaos

Arul Lakshminarayan*
Physical Research Laboratory, Navarangapura, Ahmedabad, 380009, India
(Received 26 March 1997)

Classically chaotic systems relax to coarse-grained states of equilibrium. Here we numerically study the quantization of such bounded relaxing systems, in particular the quasiperiodic fluctuations associated with the correlation between two density operators. We find that when the operators, or their Wigner-Weyl transforms, have obvious classical limits that can be interpreted as piecewise continuous functions on phase space, the variance of the fluctuations can distinguish classically chaotic and regular motions, thus providing a diagnostic device of quantum chaos. We uncover several features of the relaxation fluctuations that are shared by disparate systems thus establishing restricted universality. If we consider the nonlinearity driving the chaos as pseudotime, we find that the onset of classical chaos is indicated quantally as the relaxation of the relaxation fluctuations to a Gaussian distribution. [S1063-651X(97)14608-6]

PACS number(s): 05.45.+b, 03.65.Sq

I. INTRODUCTION

Classical dynamical systems can be classified into a hierarchy of deterministic randomness. We have well studied examples from integrable systems to Bernoulli systems, from the regular to those that are in a coarse grained manner identical to stochastic processes. An important notion in this context is that of mixing, as exemplified in the now classic ''Coke-rum'' mixture of Arnold and Avez [1]. Apart from the fundamental role it plays in deterministic randomness, alias chaos, it is the backbone of the foundations of classical statistical mechanics. While ergodicity is compatible with equilibrium, it is mixing that would ensure the drive to this state.

Quantum dynamical systems are not so neatly categorized. Quantum mixing remains a difficult notion. There are specific examples where indeed mixing can be said to occur in the configuration space, inasmuch as any two spatial wave functions decay and decorrelate exactly as classical Liouville phase space densities [2]. Yet these are rather special systems generally open and with a continuous spectra. They do not address the issue in more generic situations. The phenomenon of quantum suppression of classical chaos in diffusive systems is now well studied, and several localization mechanisms have been put forward that inhibit quantum mixing [3], yet the issues in the situation of ''hard chaos'' for bounded chaotic systems relaxing to an equilibrium have not been sufficiently addressed.

This paper studies quantum objects that are obviously connected to the twin issues of ergodicity and mixing in the classical limit. In the process we use models having a discrete spectra whose classical limit is known to be chaotic. The most convenient for our purposes is the quantization of two-dimensional area preserving maps on the torus—a much studied subject. The Hilbert space is then finite dimensional and we have fully all the contradictions between quantum and classical chaos, while retaining the attractive feature of being able to do the quantum mechanics up to machine precision and size.

Let the relevant classical phase space be Ω. This could be, for instance, the energy shell on which the Hamiltonian flow is restricted. We may formulate mixing in terms of either phase space functions or densities. Let A and B be two subsets of the phase space such that they do not intersect. Let $\chi_A(x)$ and $\chi_B(x)$ be the two characteristic functions of these subregions. Let the flow integrated for a time t be denoted by f^t, this could be a continuous flow or a discrete map. We formulate this for the case of maps in which case t is an integer. The invariant measure of the flow is denoted by μ, in the present context of area preserving maps this is simply the physical area of the phase space region.

The central quantity of interest is the correlation between the functions χ_A and χ_B. In more graphic language, as the subregion A evolves with the motion the correlation is the fractional area of its intersection with the region B. If in the long time limit this factorizes into the fraction of the areas of A and B we have mixing. In other words the fraction of A systems in B is the fractional area of B in the long time limit.

$$\mu(f^t(A)\cap B)/\mu(A)\rightarrow\mu(B)/\mu(\Omega). \tag{1.1}$$

Mixing systems are a step above ergodic ones in the hierarchy of classical dynamical systems. Ergodicity is the equality of the time average and phase space average of almost all points in the phase space. This can also be formulated as decorrelation on the average. Thus a system is ergodic if

$$\lim_{T\rightarrow\infty}\frac{1}{T}\sum_{t=1}^{T}\mu(f^t(A)\cap B)/\mu(A)=\mu(B)/\mu(\Omega). \tag{1.2}$$

Classical mixing systems are characterized by a series of complex numbers or resonances that dictate the rate of decay of correlations. Thus for purely hyperbolic or axiom A systems we can write

$$\mu(f^t(A)\cap B)/\mu(A)-\mu(B)/\mu(\Omega)=\sum_i C_i\exp(\lambda_i t). \tag{1.3}$$

*Electronic address: arul@prl.ernet.in

The λ_i are the so-called Ruelle resonances and are in general complex numbers with negative real parts independent of the particular partitions A and B. Explicit calculation of these resonances is a challenging part of dynamical systems theory; there are special models that are isomorphic to finite Markov processes for which these can be analytically found, for example, the multibaker maps [4,5].

What we wish to study below are quantities in quantum mechanics that are naturally related to the classical correlation functions defined above. In particular we will analyze the long time behavior of these functions as we expect there to be purely quantum effects in these regimes. For short times it is expected, and has been demonstrated, that the classical and quantum largely coincide [6,7]. The long-time behavior is of course very interesting because equilibrium is an asymptotic (in time) property. Just as there is ''equilibrium'' classically, a state where complete decorrelation has been practically achieved, we will study the quantum equilibrium and the associated fluctuations, which we will find has universal features in a limited manner and is often a sensitive measure of whether the classical limit is chaotic or not. The qualifications in the previous statement are necessary for reasons we will clarify below.

II. THE QUANTUM CORRELATION FUNCTION

The relevant dynamical space on quantization is a Hilbert space H_N. For regions of phase space we consider subspaces of the Hilbert space. Since we have in mind classical maps on the two torus, let the Hilbert space be of finite dimensionality N. Let there be two distinct density operators on H_N (may or may not be projection operators), P_A and P_B. We will study the cases when these operators on H_N have obvious classical limits as functions of the phase space. We will restrict ourselves initially, and largely, to the case when the operators are projection operators such that $P_A+P_B=I_N$, where I_N is the N-dimensional identity matrix. Classically this corresponds to choosing the partitions A and B such that $A\cup B=\Omega$.

We avoid assigning an operator to a general subregion of phase space, and determining whether this is possible at all (say through the Wigner-Weyl transform of the characteristic function) by restricting this study to particularly simple subspaces (or density operators) both of Ω and on H_N and going from the quantum to the classical instead of vice versa. Choosing an ''arbitrary'' subspace (or operator) of H_N obviously does not correspond to a proper subregion of the classical phase space and we will see that such subspaces do not provide interesting relaxation behaviors in that they do not distinguish between classically chaotic and regular motions. We may also construct operators out of coherent states that provide an adequate quantum equivalent of the characteristic functions. For instance, if $|z\rangle$ is the usual coherent state on the plane, we may consider

$$P_A=\int_A d^2z|z\rangle\langle z|. \tag{2.1}$$

We will finally use such operators after adapting them to the toral phase space.

If we use pure states, say $|n\rangle$, we can construct the density operators as $\Sigma|n\rangle\langle n|$. Let the dimensionality of the subspace A be $n_A=f_AN$; then $n_B=N-n_A=f_BN$. The fractions f_A and f_B determine the relative sizes of the partitions and we will assume below that $1\ll n_A,n_B\ll N$, that is, the subspaces are large enough to contain many states and be considered the quantum equivalent of a finite (much larger than $\hbar$) region of phase space. We will mostly use projection operators that are diagonal in the position basis. In this case the classical region corresponding to

$$P_A=\sum_{n=0}^{f_AN-1}|n\rangle\langle n| \tag{2.2}$$

is the rectangle $[0,f_A)\times[0,1)$ and the region corresponding to P_B is the rectangle $[f_A,1)\times[0,1)$, as the phase space is taken to be the unit torus $(q,p)=[0,1)\times[0,1)$.

We now introduce the dynamics as a unitary operator U acting on the states of H_N. The central quantity of interest is then

$$C_{AB}(t)=\mathrm{Tr}(U^tP_AU^{-t}P_B)/N, \tag{2.3}$$

which gives us the overlap of the subspace A propagated for time t with the subspace B. We may note that this is an important and natural physical quantity to study and has appeared before in several contexts, for example, Ref. [6]. It can also be viewed as an analog of Landauer conductance for bound systems and as such should be of considerable importance in quantum transport. If in fact there is factorization in time then $C_{AB}(\infty)$ must be compared with $\mathrm{Tr}(P_A)\mathrm{Tr}(P_B)/N^2=f_Af_B$. The operators U used in this paper are briefly described in the Appendix and have been essentially described before.

Since U has a discrete and finite spectrum, the correlation can only be a finite sum of purely oscillatory terms and can therefore display decay only over short time scales (of the order of Heisenberg time). The decorrelation is therefore not expected. As an extreme quantum example if we consider the case when the projection operators are constructed out of the basis functions of U the correlation is zero for all time. This is an extreme case and, for instance, it is not clear what the classical limit is of the Wigner-Weyl transform of projection operators constructed out of such a basis. We will consider ''generic'' subspaces and projection operators and any claim of universality made below has to be viewed with this caveat. We may note that this plagues random matrix theory descriptions of eigenfunctions as well, as it involves basis-dependent quantities. Here the basis dependence enters as the basis in which the projection operators are diagonal.

It was suggested earlier using quantized multibaker maps that the quantum correlation function approached the classical correlation function in the classical limit corresponding here to $N\to\infty$ [7]. Certain remarkable features of quantum relaxation were noted there including relaxation localization and effects of symmetries on transport. Here we wish to study the fluctuation properties more closely and uncover possible universal features. Therefore we study rather standard models such as the Taylor-Chirikov (standard) map [3], the kicked Harper system [9], and the baker map [10] although most of these models do not have explicit expressions

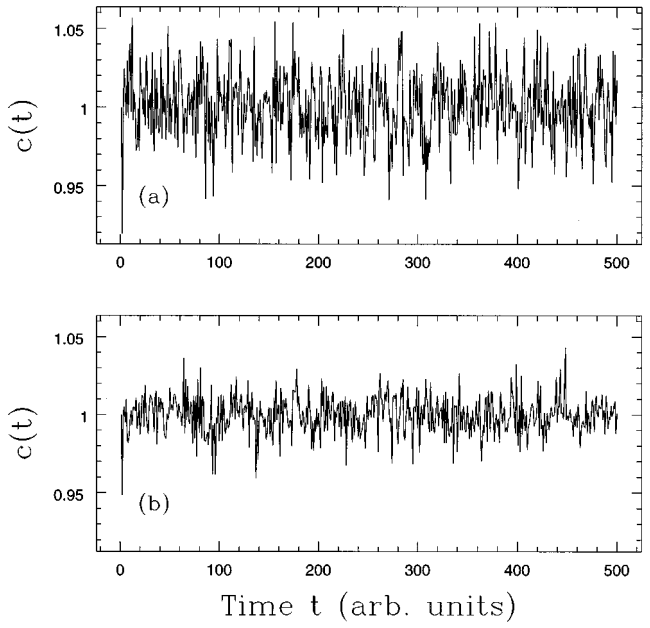

FIG. 1. The relaxation fluctuations as a function of time for the standard map with $K=20$ and (a) $N=100$ (b) $N=200$.

for the classical Ruelle resonances and are probably not axiom A systems (except the baker map). However, it is very reasonable to assume that in certain well-known parameter regimes they can be for all practical purposes mixing systems.

Normalizing the correlation so that the classical limit, if it exists, is for large times unity we study the quantity $c(t)=C_{AB}(t)/f_Af_B$, where from now on we will acknowledge implicitly the dependence of the correlation on the particular choice of partitions. Figure 1 shows an example of the generic behavior of $c(t)$, this particular data being for the standard map at two different values of the inverse Planck constant N for the same classical value of the chaos parameter. The initial relaxing behavior is not clear from the figures as the time scales are much larger than the inverse of the principal Ruelle resonance. The projection operators used are diagonal in the discrete position basis, P_A is given by Eq. (2.2), and $P_B=I_N-P_A$. The position eigenbasis is denoted as $|n\rangle$ and in this figure $f_A=f_B=1/2$.

We note that in this paper we have used dimensionless scaled position and momentum coordinates and that the time is measured as multiples of the period of the kick, taken as unity. Modulo-one conditions restrict the phase space to the unit torus so that the dimension of the Hilbert space N is related to the Planck constant as $N=1/h$ and the classical limit corresponds to $N\to\infty$ while the parameters of the map such as the kick strengths are scaled and dimensionless.

The first observation is that the quantum correlation is in fact quite close to the classical value of unity; second is that the average of the oscillations in relation to unity will give us some information about whether quantum mechanics is inhibiting transport or otherwise; third, this average must in the classical limit tend to unity, fourth is the observation that the fluctuations are getting smaller in the classical limit and must tend to zero. Some of these observations have been made and substantiated earlier [7], here we will elaborate and present more results.

Previous work on the use of time developing states to study the quantum manifestations of chaos have basically concentrated on the survival probability of a pure state [8]. This corresponds to the choice $P_A=P_B=|\psi\rangle\langle\psi|$ with an arbitrary normalized initial state $|\psi\rangle$ and thus $f_A=f_B=1/N$. Such survival probabilities averaged over random initial states show a distinct difference between chaotic and regular systems. In contrast what we study in this paper are density (or projection) operators and not pure states. It becomes quite important that f_AN and f_BN are large and are of the order of the Hilbert space dimensionality N itself. Besides any ''arbitrary'' state can be chosen for the calculation of the survival probability while we will restrict ourselves to those projection operators that can be interpreted as phase space regions in the classical limit. This is to ensure that the classical transition to chaos is fully reflected in the quantum relaxation, as will be illustrated below.

A. The average

The quantum ''equilibrium'' as opposed to the classical is a highly oscillatory state, with the fluctuations coming from the discrete nature of the spectrum. We will denote the time average of the correlation function by $\langle c\rangle$ and its variance by σ^2. These quantities can be written in terms of the eigenfunctions of the evolution operator U, which satisfy the following equation:

$$U|\psi_m\rangle=e^{iE_m}|\psi_m\rangle,\quad m=0,\ldots N-1. \tag{2.4}$$

The real numbers E_m are the eigenangles of the quantum map, and we assume that there are no exact degeneracies as is the generic case. The correlation is then

$$c(t)=\frac{1}{Nf_A(1-f_A)}\sum_{m_1,m_2}\sum_{n_1=0}^{Nf_A-1}\sum_{n_2=Nf_A}^{N-1}e^{it(E_{m_2}-E_{m_1})}\langle n_2|\psi_{m_1}\rangle \times\langle\psi_{m_1}|n_1\rangle\langle n_1|\psi_{m_2}\rangle\langle\psi_{m_2}|n_2\rangle. \tag{2.5}$$

Thus we can express the average quite simply as

$$\langle c\rangle=\frac{1}{Nf_A(1-f_A)}\sum_{m=0}^{N-1}\sum_{n=0}^{f_AN-1}\sum_{n'=f_AN}^{N-1}|\langle n|\psi_m\rangle|^2|\langle n'|\psi_m\rangle|^2. \tag{2.6}$$

Thus the average is a measure of the distribution of the eigenvectors in the subspaces A and B. We suggest that $\langle c\rangle<1$ generically, indicating a certain reluctance to participate equally in both the partitions in proportion to their sizes. Time-dependent quantum chaotic systems such as the kicked rotor on the cylinder are known to suppress classical chaos and lower diffusion [3]. The corresponding suppression in the case of bounded systems is in the average relaxation such as measured by $\langle c\rangle$. We note that the sum over n and n' expressing the average can be factored into two single sums, and we see that if, for instance, we had a parity symmetry forcing the wave function to be essentially identical in the subspaces A and B we would have $\langle c\rangle=1$, which is indeed the case for the fluctuations shown in Fig. 1. The average $\langle c\rangle$ could also be greater than unity in the presence of symmetries, or if the partition B is identical to A. Although in the absence of any special symmetry it is true that

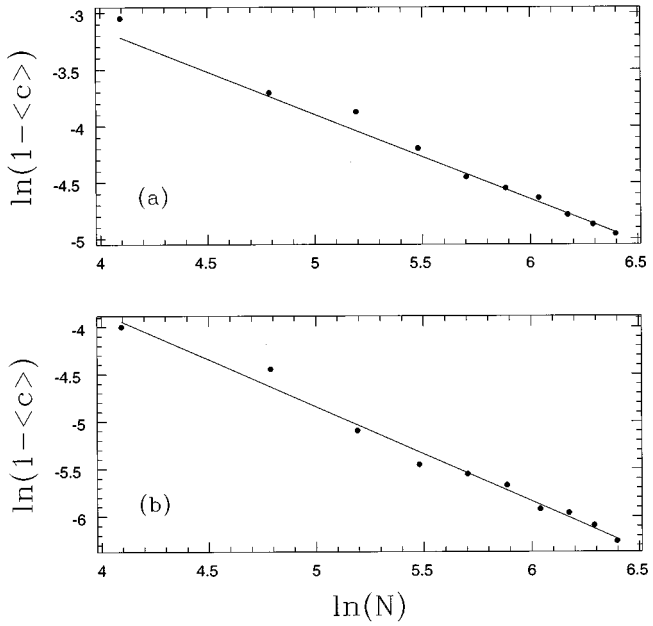

FIG. 2. The average of the fluctuations for (a) the quantum baker map quantizing the (2/3,1/3) Bernoulli scheme and (b) the standard map with $K=20$. Shown is the logarithm of the deviation from unity as a function of ln(N).

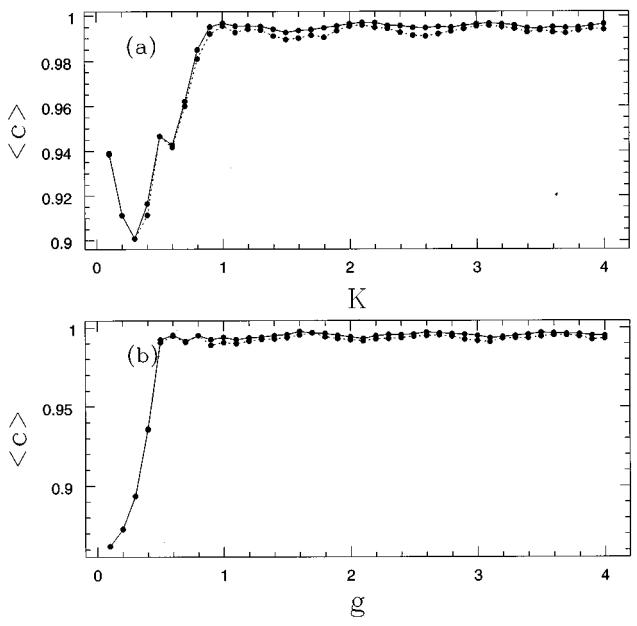

FIG. 3. The average relaxation as a function of the kicking strength for (a) the standard map, (b) the Harper map. The solid line corresponds to $N=300$ while the dotted one to $N=200$.

classical chaos will tend to enhance the average making it closer to unity, this effect is quite marginal and practically nonexistent when a transition to complete classical chaos is achieved.

Figure 2(a) shows the average for the quantized baker map implementing the Bernoulli scheme (2/3,1/3) as a function of the inverse Planck constant N. The partitions are such that $f_A=f_B=1/2$. Shown is the deviation of the average from unity and an approximate power law is observed for large N. Thus we can write

$$\langle c\rangle \sim 1-\alpha N^{-\gamma}, \tag{2.7}$$

and in this case $\gamma\approx 3/4$. The relaxation localization is implied by α being positive. Figure 2(b) shows the same quantity for the standard map and we find for the partition $f_A=1/4, f_B=3/4$ that $\gamma\approx 1$, with a different value of α. We note that in both the cases there is a small oscillation about the fitted straight line. Figure 3(a) shows the variation of the average with the classical kick parameter K for the standard map, the map undergoing a transition to complete chaos with the breaking of the last KAM torus at $K\approx 1$. The partition A was such that $f_A=1/4$ and B was the complementary space. Also illustrated is the localization effect and the same for the kicked Harper model in Fig. 3(b). The kicked Harper map, or simply the Harper map, undergoes a transition to chaos at the kick strength $g\approx 0.63$ (see Appendix).

B. The variance and the distribution

A promising candidate is the variance of the fluctuations which exist irrespective of the symmetries of the system. This can also be expressed in terms of the eigenfunctions of the system. In the particular case when $P_A+P_B=I_N$, writing for f_A simply f, we get after some simplifications

$$\sigma^2=\frac{2}{N^2 f^2(1-f)^2}\sum_{m_2>m_1}\left|\sum_{n=0}^{fN-1}\langle n|\psi_{m_2}\rangle\langle\psi_{m_1}|n\rangle\right|^4. \tag{2.8}$$

Thus the variance measures a correlation between distinct pairs of eigenfunctions. There is a coherent partial sum over Nf states that makes the variance nontrivial and perhaps nonuniversal.

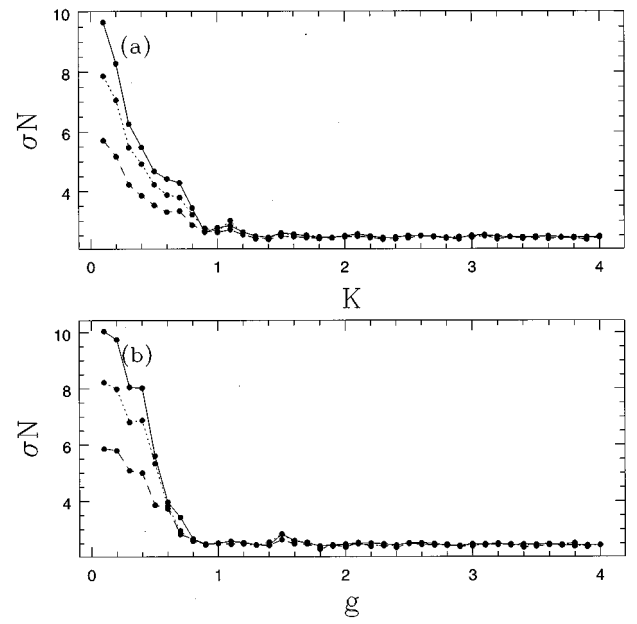

FIG. 4. The scaled standard deviation σN as a function of the kick strength for (a) the standard map, (b) the Harper map. The solid line corresponds to $N=300$, the dotted line to $N=200$ and the dashed line to $N=100$.

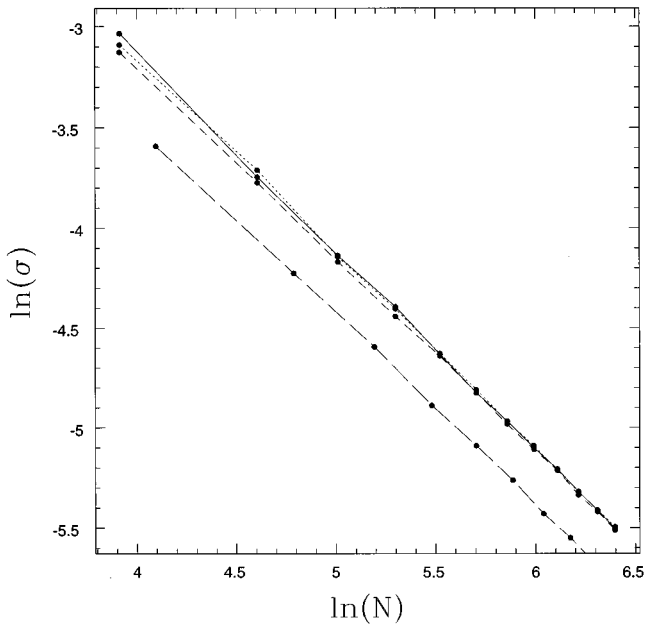

FIG. 5. The standard deviation as function of the scaled inverse Planck constant N on a logarithmic plot. The solid line corresponds to a standard map with $K=20$, the dotted line to the Harper map with $g=4$, the small dashed line to the usual symmetric quantum baker map, and the large dashed line to the unsymmetric (2/3,1/3) baker map.

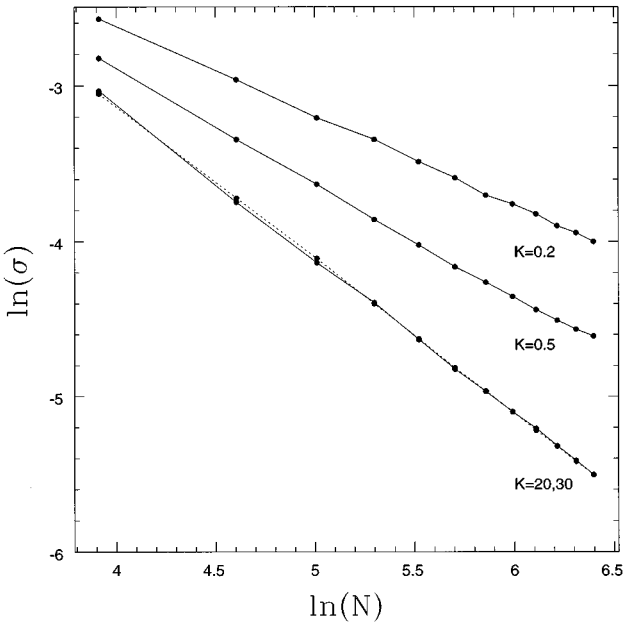

FIG. 6. Same as Fig. 5 for the standard map at different values of the kick strength K, the dashed line corresponds to $K=30$, while the solid to $K=20$.

Figure 4(a) shows the standard deviation σ scaled to σN as a function of the kick strength in the case of the standard map. The transition to classical chaos at $K\approx 1$ is visible in the variance of the fluctuations as a point at which it attains an approximately constant value. The relaxation fluctuations are therefore significantly different depending on the dynamical nature of the classical limit, being in general larger for regular systems than chaotic ones, and thus provide a novel diagnostic device for the study of quantized chaotic systems.

Figure 4(b) shows identical quantities for the case of the kicked Harper map. The variance seems to have no further dependence on measures of chaos and scales as $\hbar$ quite universally when the classical limit is chaotic. This scaling is shown explicitly in Fig. 5 for three systems in the chaotic regime: the kicked rotor, the kicked Harper map, and the usual quantum baker map. The fact that the three lines, of slope close to -1, are practically on top of each other is evidence of a limited universality of the relaxation fluctuations. The limits to universality will be discussed in the following, but also shown in the figure are the results for a generalized baker map implementing the (2/3,1/3) Bernoulli scheme, which clearly shares the same slope but is different otherwise from the other cases, which are symmetric.

When the classical limit is regular there is still evidence for scaling with $\hbar$ but with nonuniversal exponents. Thus Fig. 6 suggests that for the standard map,

$$\sigma \sim N^{-\gamma}, \tag{2.9}$$

with the exponent γ increasing to unity as the kick strength is increased to induce the transition to chaos. When $K=20$ or $K=30$ the exponent is already close to unity and the two cases are practically indistinguishable.

When $f\neq 1/2$ the relaxation is between nonsymmetrically related partitions of unequal measures. The quantum variance is studied directly as a function of f. Still we are considering the case when the two partitions complement each other. Results not shown here indicate that the dependence of the standard deviation on N (or $\hbar$) remains the same, namely, N^{-1}. Thus we may conjecture the existence of a function $g(f)$ such that $\sigma = g(f)/N$. The function $g(f)$ will naturally depend on the choice of the density operators P_A and P_B. If further we choose these operators as the projection operators described by the Eq. (2.2), we numerically find the relation

$$\sigma = \frac{\pi^2 (2f)^{\beta}}{16Nf(1-f)}, \quad 0<f\leqslant 1/2, \tag{2.10}$$

where $\beta\approx 0.83$. The constant has been identified as related to the number π by averaging over different K in the chaotic regime. Beyond $f=1/2$ symmetry of the maps ensures that $\sigma(f)=\sigma(1-f)$. It is to be emphasized that although σ is independent of model parameters like K, we are assuming that there has been a completed transition to full scale chaos.

Figure 7 compares $\sigma N f(1-f)$ with the fit $\pi^2(2f)^{\beta}/16$ for the standard map, the Harper map and the baker map. The standard map and the Harper fall practically on top of each other while the baker map shows deviations although the trend is maintained. The insensitivity of this curve to the parameter K or g indicates that once chaos is achieved the fluctuations are essentially the same. The curve σN as a function of f is thus interesting in that it has restricted universal features. The Harper and the standard maps behave almost identically while there are deviations for the baker;

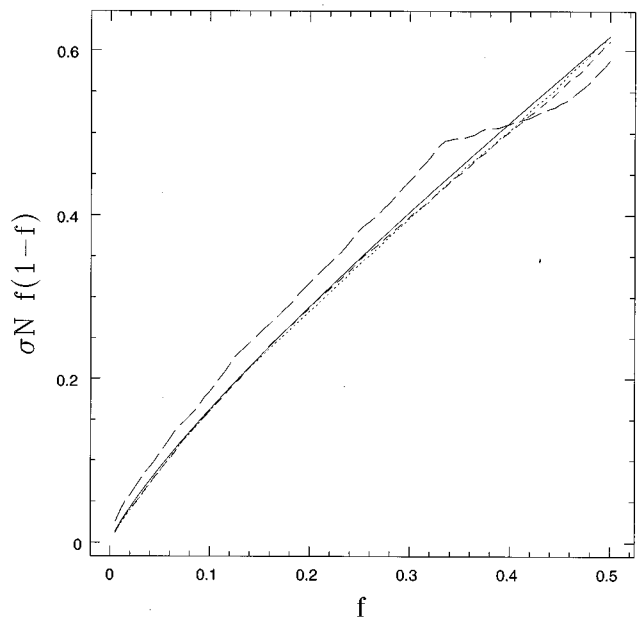

FIG. 7. The standard deviation normalized to $\sigma Nf(1-f)$ as a function of f. The solid line is the fit (see text), while the dotted line corresponds to the standard map at $K=20$, the short dashed line to the Harper map with $g=4$ and the long dashed line to the usual baker map. In all cases $N=200$.

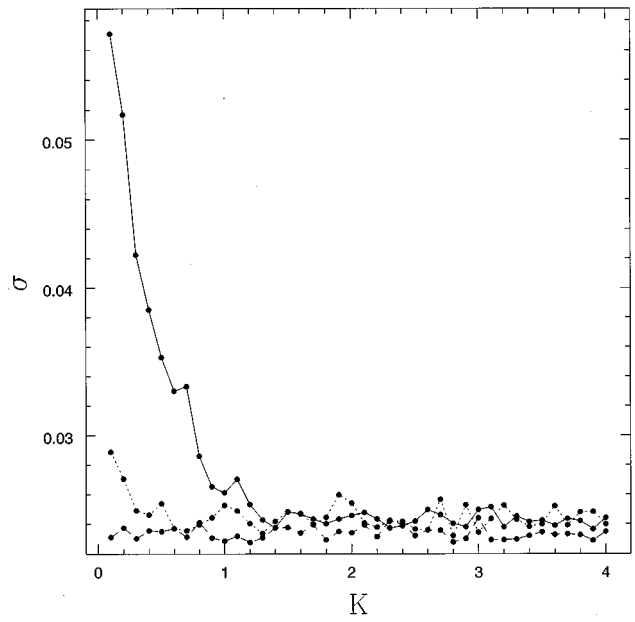

FIG. 8. The standard deviation as a function of the kick strength for the standard map with $N=200$. The dotted line corresponds to using projection operators constructed out of every alternative position basis and the dashed line to projection operators constructed out of the eigenbasis of the standard map at $K=155$. For comparison is shown the case of the usual projection operator from Fig. 4.

moreover the curve is most definitely dependent on the operators P_A and P_B, but once this is fixed the fluctuations might be model independent.

Though the fluctuations are not universal they do distinguish classically regular and chaotic motions when the operators P_A and P_B have meaningful classical limits. If this condition is violated then the fluctuations are incapable of such a separation. This is in contrast to RMT based arguments for the randomness of a wave function, where so much information is lost that in any generic basis the wave functions of a classically chaotic system are universally distributed. We will illustrate this in two ways. In the first we choose $P_A=\Sigma n_{\text{even}}|n\rangle\langle n|$ and P_B is the complementary space. Clearly in the classical limit these projection operators do not describe meaningful phase space regions. In the second we choose half the eigenbasis of the kicked rotor at $K=155$ for constructing P_A and P_B is the complementary space. Figure 8 shows that the variance does not capture the transition to chaos at around $K=1$ for the kicked rotor, unlike in the cases above, one of which has been repeated for comparison purposes. However, once the transition to chaos is complete the three standard deviations seem to coincide. We have diagonalized a standard map at $K=155$ to ensure that there are no special correlations with the system at around $K=4$.

Finally we construct the operators out of coherent states so that the interpretation as subspaces of phase space is intuitively obvious in the classical limit. We use the discrete toral coherent states developed by Saraceno [11]. Let $|m,n\rangle$ be such a state that is localized at $(q=m/N,p=n/N)$ on the unit torus. We take

$$P_A=\sum_{(q,p)\in A}|m,n\rangle\langle m,n|$$

and P_B is similarly constructed. In the computation shown below we have taken A to be the subspace $[0,1/2)\times[0,1/2)$ and B to be $[1/2,1)\times[1/2,1)$. The variance is evaluated as above with some minor differences, since $P_B\neq 1-P_A$. The measures of the quantum subspaces are $N^2/4$, as we have used normalized coherent states. The eigenfunctions are expressed in the coherent state basis and the variance is evaluated. Figure 9 shows the results of this computation and once more we recover the property that the variance captures the classical transition to chaos. Not presented are some more results, in particular the computations using the momentum basis vectors, as these simply reflect the general trends already noted above.

We have been studying the mean and standard deviation of a quantity that is truly a quasiperiodic oscillation; the distribution of such a quantity ought to be significantly different from a random process. However, Fig. 10 motivates that the effect of quantum chaos is to cast the oscillations into the ubiquitous Gaussian process, and increasingly more so in the classical limit, thereby indicating that the mean and standard deviation are sufficient to characterize the relaxation process. The solid line is a Gaussian distribution with zero mean and standard deviation equal to $\pi^2/4$, as the partitions used correspond to $f_A=f_B=1/2$. In sharp contrast Fig. 11 shows the same for the case of the standard map at $K=0.2$ when the dynamics is predominantly regular. The distribution is much broader and is also nonsymmetric. Thus if the parameter K is considered as a pseudo time variable, the onset of chaos is signaled as the realization of a stationary state of the relaxation fluctuations—the Gaussian distribution.

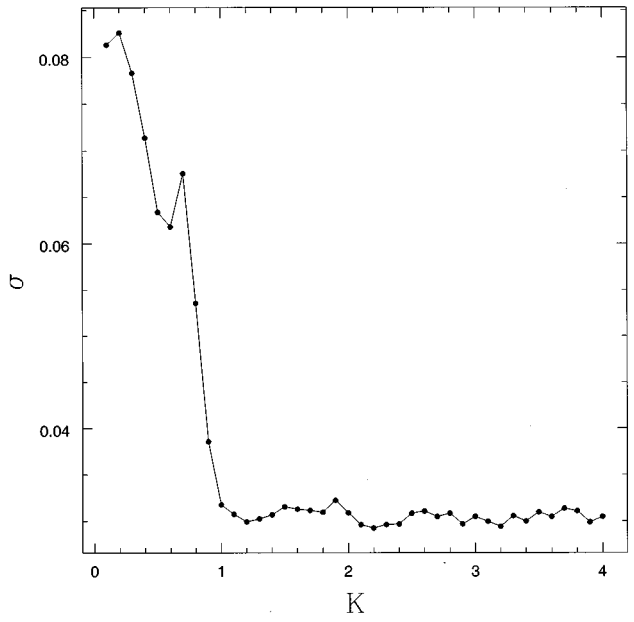

FIG. 9. The standard deviation as a function of kick strength for the standard map using the operators constructed out of toral coherent states, see text.

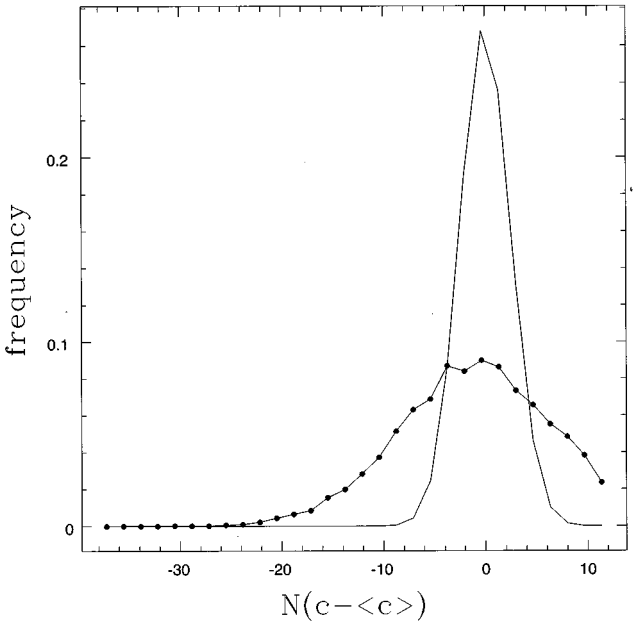

FIG. 11. Same as Fig. 10 but for the case when $K=0.2$ corresponding to predominantly regular motion. The solid line still corresponds to the same Gaussian.

III. SUMMARY

We have studied the quasiperiodic relaxation in bound quantum systems whose classical counterparts relax to a coarse grained equilibrium. We have concentrated on the correlations between density operators whose classical limits (or more correctly the limit of their Wigner-Weyl representations) may be interpreted as piecewise continuous functions on phase space. We have observed that in the absence of special symmetries the average quantum relaxation is smaller than the classical, and we have presented some scaling relations with $\hbar$.

The relaxation fluctuations have been shown to provide rather interesting characterization of the quantum motion. They sometimes have universal characteristics although these are limited. The kicked map and the Harper model with identical symmetry properties have been shown to be practically identical in the behavior of their relaxation fluctuations. The standard deviation of these fluctuations have been studied and has been shown to decrease to a constant value with a rather sharp change in the values corresponding to the transition to chaos in the classical system. Thus the fluctuations provide a way to characterize quantum chaos. The standard deviation has been shown to scale as $\hbar$ when there is classical chaos universally, while it has other nonuniversal power law dependencies when the classical motion is not chaotic.

Random matrix theories have been providing a framework to study several properties of quantized chaotic systems and it is natural to explore the random matrix predictions for the quantities studied in this note. It is of special interest to place the numerical results in this paper in the context of a generalization of the previous work on survival probabilties [8] and work on these aspects is currently underway.

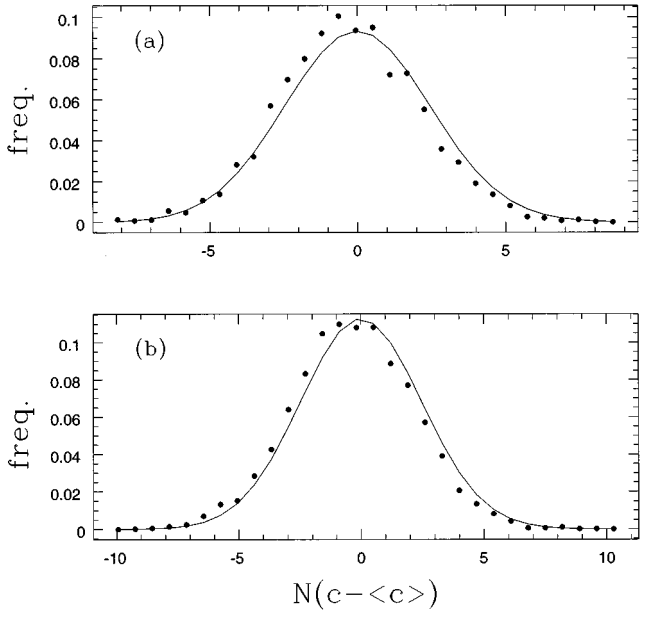

FIG. 10. The distribution of the relaxation fluctuations using the first 5000 $c(t)$ values for the standard map with $K=20$ and (a) $N=100$ (b) $N=200$. The solid line corresponds to a Gaussian distribution.

APPENDIX

The Taylor-Chrikov, or the standard map, or the kicked rotor, used in this paper is described below [3,12]. Let the classical map be $[q_{t+1}=q_t+p_{t+1},\quad p_{t+1}=p_t-V'(q_{t+1})]$, both q and p taken mod 1. V' is the derivative of the kicking potential, which is assumed to have unit periodicity. The toral states are assumed to satisfy certain boundary conditions specified by a point on the dual torus. Let $|q_n\rangle$ and $|p_m\rangle$ be the position and momentum states then $|p_{m+N}\rangle=e^{-2\pi ia}|p_m\rangle$ and $|q_{n+N}\rangle=e^{2\pi ib}|q_n\rangle$, where (a,b)

are real numbers between 0 and 1; N is the dimensionality of the Hilbert space. If $b=0$, upon canonical quantization we get the finite unitary operator

$$U_{n,n'}=\frac{e^{i\pi/4}}{\sqrt{N}}\exp\left[-2\pi iNV\left(\frac{n+a}{N}\right)\right]\exp\left(i\frac{\pi}{N}(n-n')^2\right). \tag{A1}$$

In this paper we have used for the standard map $V(q)=K\cos(2\pi q)/(2\pi)$, and $a=1/2$ which makes the quantum map possess an exact parity symmetry about $q=1/2$. The values of N are restricted to the even integers.

The kicked Harper map [9] on the torus is similar to the above system except for the momentum dependence. If the Hamiltonian is

$$H=V_1(p)\ +\ V_2(q)\sum_{n=-\infty}^{\infty}\delta(t-n),$$

the quantum map is

$$U_{n,n'}=\frac{1}{N}\exp\left[-2\pi iNV_2\left(\frac{n+a}{N}\right)\right]\sum_{m=0}^{N-1}\times\exp\left[-2\pi iNV_1\left(\frac{m+b}{N}\right)\right]\times\exp\left(\frac{2\pi i}{N}(m+b)(n-n')\right). \tag{A2}$$

For the Harper map used in this paper we have taken $(a=b=1/2)$, $V_1(p)=-g_1\cos(2\pi p)/(2\pi)$ and $V_2(q)=-g_2\cos(2\pi q)/(2\pi)$. This set once again ensures symmetry properties of the quantum map. The classical map is $[q_{t+1}=q_t+g_1\sin(2\pi p_{t+1}),\ \ p_{t+1}=p_t-g_2\sin(2\pi q_t)]$, again the mod 1 rule is assumed. If $g_{1,2}$ are equal, as assumed in this paper, the transition to chaos occurs around $g_{1,2}=0.63$. In both the kicked Harper model and the rotor the time between kicks has been taken as unity, as anyway there are two parameters in the quantum problem, the scaled Planck constant N and the kick strength (K or g).

The baker map [10,11] comes in several varieties. It has been shown that the usual baker map $[(q_{t+1}=2q_t,\ \ p_{t+1}=p_t/2)$ if $0<q_t<1/2$ and $(q_{t+1}=2q_t-1,\ \ p_{t+1}=(p_t+1)/2)$ if $1/2<q_t<1]$ is isomorphic to the (1/2,1/2) Bernoulli process. The quantum baker map on the torus is then the unitary operator

$$U=G_N^{-1}\begin{pmatrix}G_{N/2} & 0\\ 0 & G_{N/2}\end{pmatrix}, \tag{A3}$$

where G_N is the finite Fourier transform matrix with elements

$$(G_N)_{m,n}=\frac{1}{\sqrt{N}}\exp(-2\pi i(m+1/2)(n+1/2)/N).$$

We have assumed antiperiodic boundary conditions $(a=b=1/2)$ as this is known to preserve classical symmetries.

The generalized baker map used in this paper is a dynamical system implementing the (2/3,1/3) Bernoulli process and is the classical map $((q_{t+1}=3q_t/2,\ p_{t+1}=2p_t/3)$ if $0<q_t<2/3$ and $[q_{t+1}=3q_t-2,\ p_{t+1}=(p_t+2)/3]$ if $2/3<q_t<1)$. The quantum map is the unitary operator

$$U=G_N^{-1}\begin{pmatrix}G_{2N/3} & 0\\ 0 & G_{N/3}\end{pmatrix}. \tag{A4}$$

[1] V. I. Arnold and A. Avez, *Ergodic Problems of Classical Mechanics* (Benjamin, New York, 1968).

[2] S.Weigert in *Adriatico Research Conference and Miniworkshop, Quantum Chaos*, edited by H. A. Cerdeira, R. Ramaswamy, M. C. Gutzwiller, and G. Casati (World Scientific, Singapore, 1990).

[3] F. M. Izrailev, Phys. Rep. **196**, 299 (1990).

[4] Y. Elskens and R. Kapral, J. Stat. Phys. **38**, 1027 (1985).

[5] P. Gaspard, J. Stat. Phys. **68**, 673 (1992).

[6] O. Bohigas, S. Tomsovic, and D. Ullmo, Phys. Rep. **233**, 45 (1993).

[7] A. Lakshminarayan, and N. L. Balazs, J. Stat. Phys. **77**, 311 (1994).

[8] F. Leyvraz *et al.*, Phys. Rev. Lett. **67**, 2921 (1991); Y. Alhassid and N. Whelan, *ibid.* **70**, 572 (1993); A. Tameshtit and J. E. Sipe, Phys. Rev. A **45**, 8280 (1992); J. Wilkie and P. Brumer, Phys. Rev. Lett. **67**, 1185 (1991).

[9] P. Leboeuf *et al.*, Phys. Rev. Lett. **65**, 3076 (1990).

[10] N. L. Balazs and A. Voros, Ann. Phys. (N.Y.) **190**, 1 (1989).

[11] M. Saraceno, Ann. Phys. (N.Y.) **199**, 37 (1990).

[12] S.J. Chang and K. J. Shi, Phys. Rev. Lett. **55**, 269 (1985).